

## Phenomenology of extra $E_6$ neutral gauge bosons in $ep$ collisions

Simon Capstick

*Department of Theoretical Physics, Oxford University, 1 Keble Road, Oxford OX1 3NP\**  
*and Department of Physics, University of Toronto, Toronto, Canada M5S 1A7*

Stephen Godfrey

*Physics Department, Brookhaven National Laboratory, Upton, New York 11973\**  
*and TRIUMF, 4004 Wesbrook Mall, Vancouver, Canada V6T 2A3*

(Received 4 February 1987)

We have studied the effects of an extra  $Z^0$  boson expected from  $E_6$  grand unified theories on cross sections and asymmetries in electron-proton collisions at DESY HERA. Such measurements were found to be more sensitive to the effects of an extra  $E_6$   $Z^0$  boson than analogous experiments at  $e^+e^-$  colliders for a large range of allowed  $Z'$  parameters. In the event that evidence for an extra  $Z^0$  boson was found at  $e^+e^-$  colliders, measurements at HERA would be necessary to determine its properties and its place in theory. We note that the deviations from the standard model allowed by existing neutral-current data are substantial.

### I. INTRODUCTION

Recently, there has been a resurgence of interest in  $E_6$  grand unified theories (GUT's) due to the possibility that they may be the low-energy limit of superstring theories.<sup>1-3</sup> Although at present it is not clear what aspects of these theories will survive it is still interesting to study their phenomenology, not only for the specific predictions of the models, but also as exercises in interpreting new physics which might be observed at the next generation of particle accelerators. From this perspective there has been much interest in the phenomenological possibilities of  $E_6$  GUT's including the production and detection of the exotic fermions of  $E_6$  (Ref. 4) and of the extra gauge bosons expected in  $E_6$  (Ref. 5). Although it is not clear if exotic low-mass fermions exist in superstring theories, one common feature of superstring-motivated  $E_6$  theories is the existence of extra neutral gauge bosons. With this motivation, numerous groups have studied the constraints which the present experimental data puts on the existence of extra  $Z^0$ 's (Refs. 6-9), the effects of extra  $Z^0$ 's in  $p\bar{p}$  colliders,<sup>10</sup> and in the next generation of  $e^+e^-$  colliders.<sup>11-15</sup> Because of this widespread interest in extra  $Z^0$ 's, which we denote  $Z'$ 's, it is interesting to compare the experimental *reach* of the various experiments, which we define to be the highest  $Z'$  mass which a given experiment can detect, of both existing experiments and of future experiments. With this motivation we will extend the previous analysis of extra  $Z^0$ 's to the phenomenology of  $ep$  collisions such as at DESY HERA.<sup>16</sup>

Our goal here is twofold: first, we wish to study how cross sections and asymmetries will vary with the parameters of the extended model; the extra  $Z^0$ 's couplings to fermions, the mass of the  $Z'$ , and the magnitude of the  $Z_{SM}^0$ - $Z_{E_6}^0$  mixing; second, we wish to compare the *reach* of  $ep$  colliders with the bounds from existing neutral-current data and the *reach* of the next generation of  $e^+e^-$

colliders. In the latter, it was previously found that the asymmetries in  $e^+e^-$  collisions allowed by present phenomenology are quite large and such measurements could be our first hint of new physics beyond the standard model.<sup>12</sup> In this paper we study the size of the asymmetries which are allowed at HERA,<sup>17</sup> although we point out that the bounds we use here will no doubt be revised by future measurements at the Stanford Linear Collider (SLC) and CERN LEP.

The outline of the paper is as follows. We begin in Sec. II with a very brief sketch of some relevant  $E_6$  group theory to define our notation with respect to the  $Z'$  couplings. In Sec. III we give the expression for the doubly differential  $ep$  cross section with an extra  $Z^0$  boson and the definition of the various asymmetries, followed by examples which show how these quantities will vary with different values of the  $Z'$  parameters. We also discuss the issue of statistics and the approach one might take to enhance the detection of extra  $Z^0$ 's. We summarize our results with a comparison of the *reach* of HERA in detecting  $Z'$ 's to that of the various  $e^+e^-$  colliders and the bounds from existing neutral-current data. We conclude in Sec. IV with some general comments comparing the relative merits of  $e^+e^-$  and  $ep$  colliders in searching for  $Z'$ 's and studying their properties.

### II. SOME $E_6$ CONSIDERATIONS

In this section we follow Ref. 12 to describe the parameters of the model, in particular the couplings of fermions to the extra  $Z^0$  boson which we denote the  $Z'$ . As in Ref. 12 we describe the charge of the  $Z'$  in terms of the U(1) charges of the subgroup chain

$$E_6 \rightarrow \text{SO}(10) \times \text{U}(1)_\psi \rightarrow \text{SU}(5) \times \text{U}(1)_\chi \times \text{U}(1)_\psi, \quad (1)$$

where the  $\text{SU}(3)_c \times \text{SU}(2)_L \times \text{U}(1)_{Y_W}$  groups of the standard model (SM) are embedded in SU(5). Thus, we can

TABLE I. The charges of the conventional fermion for the extra  $Z^0$  boson of  $E_6$ . The second- and third-generation fermions have the same charges as the corresponding first-generation fermions.

Fermion	$C_L^{E_6}$	$C_R^{E_6}$
$l$	$\frac{3}{2\sqrt{10}} \cos\theta_{E_6} + \frac{1}{2\sqrt{6}} \sin\theta_{E_6}$	$\frac{1}{2\sqrt{10}} \cos\theta_{E_6} - \frac{1}{2\sqrt{6}} \sin\theta_{E_6}$
$\nu$	$\frac{3}{2\sqrt{10}} \cos\theta_{E_6} + \frac{1}{2\sqrt{6}} \sin\theta_{E_6}$	$\frac{5}{2\sqrt{10}} \cos\theta_{E_6} - \frac{1}{2\sqrt{6}} \sin\theta_{E_6}$
$u$	$-\frac{1}{2\sqrt{10}} \cos\theta_{E_6} + \frac{1}{2\sqrt{6}} \sin\theta_{E_6}$	$\frac{1}{2\sqrt{10}} \cos\theta_{E_6} - \frac{1}{2\sqrt{6}} \sin\theta_{E_6}$
$d$	$-\frac{1}{2\sqrt{10}} \cos\theta_{E_6} + \frac{1}{2\sqrt{6}} \sin\theta_{E_6}$	$-\frac{3}{2\sqrt{10}} \cos\theta_{E_6} - \frac{1}{2\sqrt{6}} \sin\theta_{E_6}$

write the  $Q'$  charges in terms of  $Q_\psi$  and  $Q_\chi$  whose operators are orthogonal to those of  $Q_{EM}$  and that of the standard-model  $Z^0$ :

$$Q' = Q_\chi \cos\theta_{E_6} + Q_\psi \sin\theta_{E_6}, \quad (2a)$$

$$Q'' = -Q_\chi \sin\theta_{E_6} + Q_\psi \cos\theta_{E_6}. \quad (2b)$$

In this notation  $\theta_{E_6}=0$  corresponds to the extra  $Z^0$  in  $SO(10)$ ,  $\theta_{E_6}=90^\circ$  corresponds to the extra  $Z^0$  in  $E_6$ , and  $\tan\theta_{E_6} = -(\frac{5}{3})^{1/2}$  corresponds to the extra  $Z^0$  obtained when  $E_6$  is broken via a non-Abelian discrete symmetry to a rank-5 group.<sup>3</sup> In practice we consider only the minimal case of one extra neutral gauge boson assuming that in the case of a rank-6 group where two extra  $Z^0$ 's are present one is sufficiently heavy that its effects are suppressed for the energies considered in this paper. The quantum numbers and  $Z'$  couplings of the conventional fermions are given in Table I.

The  $Z'$  can also mix with the standard model  $Z^0$  so that the physical fields  $Z_p^0$  and  $Z_p'$  are linear combinations of the gauge fields  $Z_{SM}^0$  and  $Z_{E_6}'$  with mixing angle  $\phi$ . This mixing will alter the fermions' coupling to the  $Z^0$ 's to

$$C_{L,R} = C_{L,R}^{SM} \cos\phi + (g_{Z'}/g_{Z^0}) C_{L,R}^{E_6} \sin\phi, \quad (3a)$$

$$C'_{L,R} = -(g_{Z^0}/g_{Z'}) C_{L,R}^{SM} \sin\phi + C_{L,R}^{E_6} \cos\phi, \quad (3b)$$

where  $C_{L,R}^{SM}$  are the standard-model couplings to the  $Z^0$  given by  $C_{L,R}^{SM} = (I_{3L} - Q \sin^2\theta_W)$  and  $C_{L,R}^{E_6}$  are the left- and right-handed  $Z'$  charges given in Table I. In general  $\phi$  will be determined by a specific model as in the case of Ref. 14, but here we will treat it as a free parameter to be constrained by experiment. Since  $\phi$  comes from the diagonalization of the  $Z^0$ - $Z'$  mass matrix it can be expressed in terms of the standard-model prediction for the  $Z^0$  mass

$M_{SM} = M_W \cos^2\theta_W$  and the physical  $Z^0$  and  $Z'$  masses:<sup>18</sup>

$$\tan^2\phi = \frac{M_{SM}^2 - M_{Z_p'}^2}{M_{Z_p'}^2 - M_{SM}^2}. \quad (4)$$

With an accurate measurement of the physical  $Z^0$  mass  $\phi$  will be related to  $M_{Z'}$  and can therefore be removed as a free parameter. However, for the present, with the uncertainty in the  $Z^0$  mass, we leave  $M_{Z'}$  and  $\phi$  as two independent parameters. This results in the effective neutral-current Lagrangian

$$L_{NC} = -g_{Z^0} Z_\mu^0 J_{Z^0}^\mu - g_{Z'} Z'_\mu J_{Z'}^\mu, \quad (5)$$

where the currents are given by  $J^\mu = \sum_f C_L^f \bar{f} \gamma^\mu f$  with the sum over left-handed fermion fields.

Thus in addition to the parameters of the standard model we have four phenomenological parameters to be determined. These are  $M_{Z'}$  (the mass of the  $Z'$ ),  $\phi$  (the  $Z_{SM}^0$ - $Z_{E_6}'$  mixing angle),  $\theta_{E_6}$  (the  $Q_\chi$ - $Q_\psi$  mixing angle), and  $g_{Z'}/g_{Z^0}$  (the ratio of the  $Z^0$  and  $Z'$  coupling constants). From renormalization-group arguments<sup>19</sup> one finds that  $(g_{Z'}/g_{Z^0})^2 \leq \frac{5}{3} \sin^2\theta_W$  with the exact value dependent on the symmetry-breaking scheme. Here we will use the equality, which results when all  $U(1)$  groups are broken at the same unification mass.

### III. CROSS SECTIONS, ASYMMETRIES, AND RESULTS

In calculating deviations from the standard model in  $ep$  collisions which arise from the extra  $Z^0$ 's of  $E_6$  we begin by calculating the differential cross section for the  $t$ -channel gauge-boson-exchange process shown in Fig. 1. This results in the following cross section for a left-handed polarized electron and unpolarized proton:

$$\frac{d\sigma(e_L^- p)}{dx dy} = \frac{2\pi\alpha^2}{sx^2y^2} \sum_q \{x f_q(x, Q^2) [ |b_{LL}|^2 + |b_{LR}|^2(1-y)^2 ] + x f_{\bar{q}}(x, Q^2) [ |b_{LR}|^2 + |b_{LL}|^2(1-y)^2 ] \} \quad (6)$$

and for a left-handed polarized positron and unpolarized proton:

$$\frac{d\sigma(e_L^+ p)}{dx dy} = \frac{2\pi\alpha^2}{sx^2y^2} \sum_q \{x f_q(x, Q^2) [ |b_{RL}|^2 + |b_{RR}|^2(1-y)^2 ] + x f_{\bar{q}}(x, Q^2) [ |b_{RR}|^2 + |b_{RL}|^2(1-y)^2 ] \}, \quad (7)$$

where the sum runs over quark flavors.  $f_q(x, Q^2)$  and  $f_{\bar{q}}(x, Q^2)$  are the quark and antiquark distribution function  $Q^2 = xys$ , and  $x$  and  $y$  are the usual scaling variables,  $x = Q^2/2p \cdot q$ ,  $y = p \cdot q/p \cdot k$ .

The functions  $b_{ij}$  are given by

$$b_{ij} = \left[ -Q_q + \frac{C_i^e C_j^q}{\sin^2 \theta_W \cos^2 \theta_W} \frac{Q^2}{Q^2 + M_{Z^0}^2} + \left( \frac{g_{Z'}}{g_{Z^0}} \right)^2 \frac{C_i^e C_j^q}{\sin^2 \theta_W \cos^2 \theta_W} \frac{Q^2}{Q^2 + M_{Z'}^2} \right], \quad (8)$$

where  $Q_q$  denotes the quark electric charge and  $C_{L,R}$  and  $C'_{L,R}$  are the left- and right-handed  $Z^0$  and  $Z'$  charges given by (3a) and (3b). To obtain the cross section for right-handed electrons and positrons make the substitution  $L \leftrightarrow R$ .

In our numerical results we use the values  $M_{Z^0} = 92.5$  GeV,  $\sin^2 \theta_W = 0.229$  (Ref. 20),  $\alpha_{EM}^{-1}(M_W) = 128.5$ , and the Eichten-Hinchliffe-Lane-Quigg structure functions (set 2) given in Ref. 21. Note that Durkin and Langacker found that  $\sin^2 \theta_W$  was not sensitive to the value of  $\theta_{E_6}$  used in a fit of low-energy data even when  $Z^0$ - $Z'$  mixing effects were included. We do not include detector-dependent radiative corrections such as bremsstrahlung off the initial or final legs and virtual graphs in our calculations since they will depend on detector properties and therefore are best included by experimentalists via Monte Carlo simulations.

In what follows we explore how deviations from the standard model caused by an extra  $Z^0$  boson vary with the phenomenological parameters of the model and how one can best observe the effects of  $Z'$ 's. We find that the most important factor in observing and interpreting such deviations at HERA will be collecting sufficient statistics and as a result we will pay special attention to this issue. Although experimentalists will be far more sophisticated in their analysis of the data we believe that our results and conclusions provide a reasonable starting point in looking for the effects of extra  $Z^0$  bosons in  $ep$  collisions.

Because the issue of statistics is so crucial to the discovery of  $Z'$ 's we give in Fig. 2 the standard-model differential cross sections as a function of  $y$  for  $s = 64\,000$  GeV<sup>2</sup> and  $s = 98\,600$  GeV<sup>2</sup> so that one can appreciate the origin of the relatively large statistical errors. This sets the scale of the cross section used to obtain our error estimates. The value  $s = 98\,600$  GeV<sup>2</sup> represents the maximum center-of-mass energy at HERA, where the lumi-

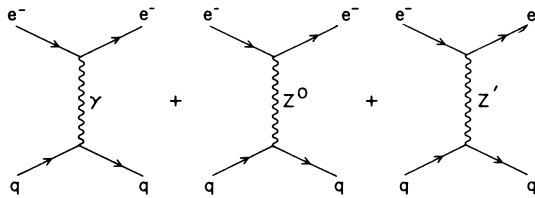


FIG. 1.  $t$ -channel processes which contribute to the  $eq$  neutral-current cross section.

osity is expected to be  $1.5 \times 10^{31}$  cm<sup>-2</sup>sec<sup>-1</sup>. At  $s = 64\,000$  GeV<sup>2</sup> one gains a factor of 6 in luminosity and we have found that an increase in luminosity is far more useful in looking for the effects of extra  $Z^0$ 's than an increase in energy. In this plot we have integrated over the  $x$  variable from 0.1 to 1.0. The lower bound was chosen as a compromise between the high statistics but small deviations at low  $x$  and the low statistics but larger deviations at high  $x$ . For example, if one lowers  $x_{\min}$  the deviations tend to get swamped by the high statistics of the low- $x$  kinematics region where the deviations are small. On the other hand, if one raises the value of  $x_{\min}$  the deviations are larger but the statistical significance is not improved because of the lower event rate. Hence our chosen compromise.

In Fig. 3 we study how the cross section varies with the parameters of the extended model. In Fig. 3(a) we plot the deviations from the standard model for the  $e^-p$  cross section as a function of  $\theta_{E_6}$  with  $\phi = 0$  and  $M_{Z'} = 150, 250$ , and 350 GeV at  $s = 64\,000$  GeV<sup>2</sup> and where we have integrated both  $x$  and  $y$  from 0.1 to 1. Note that the sensitivity of the results to extra  $Z^0$ 's is highly dependent on the value of  $\theta_{E_6}$  and hence the specific symmetry breakdown of  $E_6$ . In Fig. 3(b) we plot the same cross section, this time setting  $\theta_{E_6} = \theta_\eta$  and varying  $\phi$  from  $-0.2$  to  $+0.2$ . In both cases we show error bars which we esti-

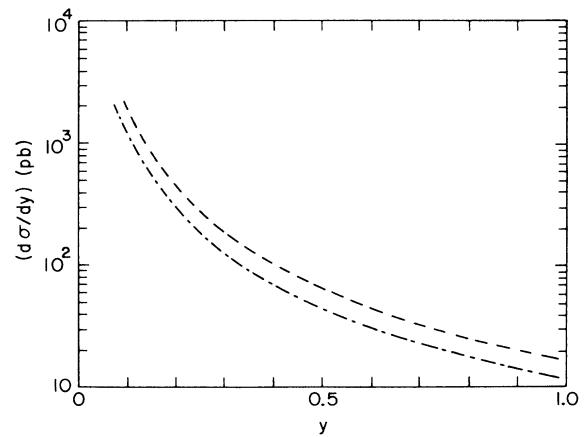


FIG. 2. The standard-model differential cross section  $d\sigma(e^-p \rightarrow e^-X)/dy$  as a function of  $y$  obtained by integrating  $x$  from 0.1 to 1.0. The dashed line is for  $s = 64\,000$  GeV<sup>2</sup> and the dot-dash line is for  $s = 98\,600$  GeV<sup>2</sup>.

mate using an integrated luminosity of  $600 \text{ pb}^{-1}$  per polarization. One can see that deviations caused by the extra  $Z'^0$ s of  $E_6$  will be observable for a  $Z'$  of several hundred GeV. In Fig. 4 we plot the deviations from the standard model for the differential cross section  $d\sigma/dy$  as a function of  $y$  for  $\theta_{E_6} = \theta_\eta$  and  $\phi = 0$  for several values of  $M_{Z'}$ , where  $\delta\sigma = \sigma - \sigma_{SM}$ . The error bars were determined by integrating  $d\sigma/dy$  over  $y$  for bins of width 0.3 centered at 0.25, 0.55, and 0.85 with an integrated luminosity of  $600 \text{ pb}^{-1}$  per polarization. As expected the smaller  $M_{Z'}$ , the larger the deviation from the standard model. In Fig. 5 we plot deviations in the differential cross section  $d\sigma/dy$

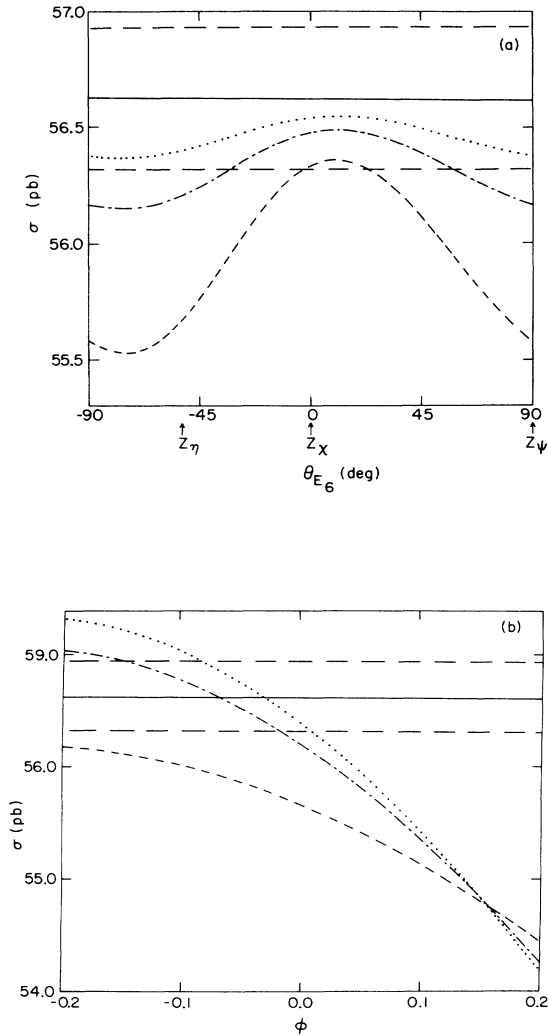


FIG. 3.  $\sigma(e^-p \rightarrow e^-X)$  for  $s = 64000 \text{ GeV}^2$  and  $\phi = 0$  obtained by integrating both  $x$  and  $y$  from 0.1 to 1.0. (a)  $\sigma$  as a function of  $\theta_{E_6}$  for  $\phi = 0$  and (b)  $\sigma$  as a function of  $\phi$  for  $\theta_{E_6} = \theta_\eta$ . In both cases the solid line is the standard-model result with the long-dashed lines representing  $1\sigma$  deviations from the standard model assuming an integrated luminosity of  $600 \text{ pb}^{-1}$  per polarization. The dashed line is for  $M_{Z'} = 150 \text{ GeV}$ , the dot-dash line is for  $M_{Z'} = 250 \text{ GeV}$ , and the dotted line is for  $M_{Z'} = 350 \text{ GeV}$ .

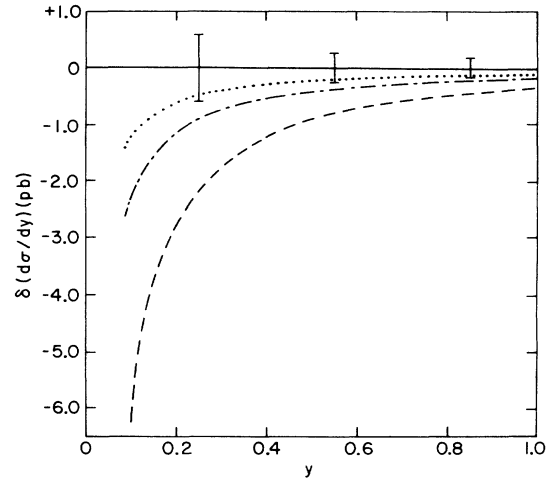


FIG. 4.  $\delta(d\sigma(e^-p \rightarrow e^-X)/dy)$  obtained by integrating  $x$  from 0.1 to 1.0 at  $s = 64000 \text{ GeV}^2$  for  $\theta_{E_6} = \theta_\eta$  and  $\phi = 0$ . The dashed line is for  $M_{Z'} = 150 \text{ GeV}$ , the dot-dash line is for  $M_{Z'} = 250 \text{ GeV}$ , and the dotted line is for  $M_{Z'} = 350 \text{ GeV}$ . The error bars were obtained by integrating  $y$  over bins of width 0.3 centered at 0.25, 0.55, and 0.85 with an integrated luminosity of  $600 \text{ pb}^{-1}$  per polarization.

as a function of  $y$  for several representative sets of parameters which are allowed by the present low-energy neutral-current data as obtained by Durkin and Langacker<sup>7</sup> with the errors determined as in Fig. 4. One can see that the deviations allowed by current data can be quite large although we expect that the present limits will be al-

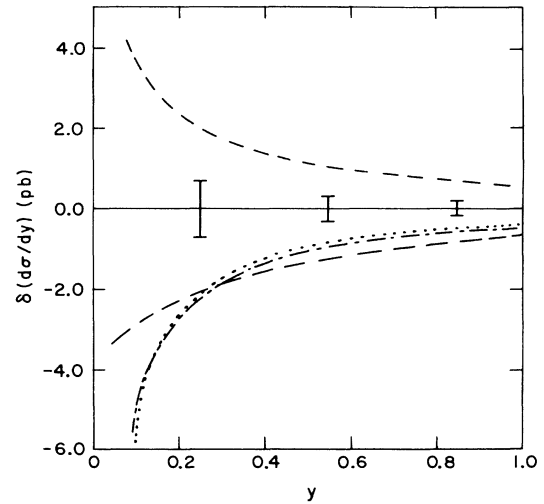


FIG. 5.  $\delta(d\sigma(e^-p \rightarrow e^-X)/dy)$  obtained as in Fig. 4 for representative parameter sets allowed by present experimental bounds. The dotted line is for  $\theta_{E_6} = \theta_\eta$ ,  $M_{Z'} = 200 \text{ GeV}$ , and  $\phi = 0.04$ , the dot-dash line is for  $\theta_{E_6} = \theta_\eta$ ,  $M_{Z'} = 120 \text{ GeV}$ , and  $\phi = -0.25$ , the short-dashed line is for  $\theta_{E_6} = \theta_\chi$ ,  $M_{Z'} = 260 \text{ GeV}$ , and  $\phi = -0.08$ , and the long-dashed line is for  $\theta_{E_6} = \theta_\psi$ ,  $M_{Z'} = 140 \text{ GeV}$ , and  $\phi = 0.06$ . The error bars are obtained as in Fig. 4.

tered by future results including those at LEP and SLC.

We next turn to the six asymmetries which can be constructed with polarized electron and positron beams:  $e_L^- - e_R^-$ ,  $e_L^- - e_R^+$ ,  $e_R^- - e_L^+$ ,  $e_L^+ - e_R^+$ ,  $e_R^+ - e_L^-$ , and  $e_L^- - e_L^+$ , where the asymmetry  $\alpha - \beta$  is defined as

$$A = \frac{\sigma(\alpha) - \sigma(\beta)}{\sigma(\alpha) + \sigma(\beta)}. \quad (9)$$

We start by showing in Fig. 6 the deviations from the standard model of the asymmetries as a function of  $\theta_{E_6}$ , where  $d\sigma/dx dy$  was integrated over both  $x$  and  $y$  from 0.1 to 1.0 and  $\delta A = A - A_{SM}$ . The errors for the asymmetries were found using<sup>16</sup>

$$\delta = \frac{1 - A^2}{\sqrt{1 - A}} \frac{1}{\sqrt{2N(\alpha)}},$$

where  $A$  is the asymmetry  $N(\alpha) = L\sigma(\alpha)$  with  $L = 600 \text{ pb}^{-1}$ . Note that the various asymmetries have different dependencies on  $\theta_{E_6}$  so that where one asymmetry may be relatively insensitive to the  $Z'$ , another asymmetry may still show measurable deviations. Thus, taken together, we find that the asymmetry measurements will be sensitive to  $Z'$ 's of several hundred GeV for most values of  $\theta_{E_6}$ . In Fig. 7 we look at the deviations of the asymmetries as a function of  $\phi$  for  $\theta_{E_6} = \theta_\eta$  and find that the deviations can be quite substantial with  $Z'$ 's of mass greater than 500 GeV being measurable except for very small values of  $\phi$ . In Fig. 8 we show how the asymmetries vary as a function of  $y$  for  $\theta_{E_6} = \theta_\eta$ ,  $\phi = 0$ , and several values of  $M_{Z'}$  where the error was determined using the same binning procedure as in Figs. 4 and 5. In the final figure of this sequence, Fig. 9, we show asymmetries for some representative parameter sets allowed by neutral-current data. They are found to be large compared to the expected statistical errors so it is possible that HERA could observe the effects of a  $Z'$  that has thus far eluded observation in low-energy neutral-current data.

So far we have shown how  $ep$  cross sections and asym-

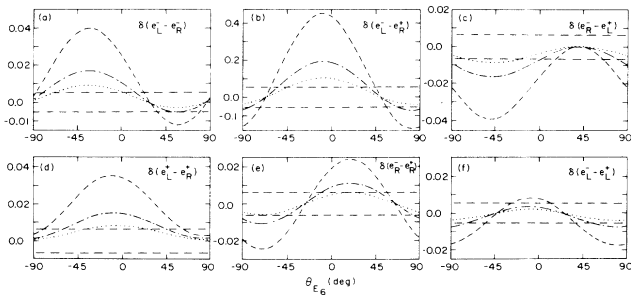


FIG. 6. Deviations from the standard model for the various  $ep$  asymmetries  $\delta(\alpha - \beta)$  as a function of  $\theta_{E_6}$  for  $\phi = 0$  at  $s = 64000 \text{ GeV}^2$  obtained by integrating  $d\sigma/(dx dy)$  over  $x$  and  $y$  from 0.1 to 1. The short-dashed line is for  $M_{Z'} = 150 \text{ GeV}$ , the dot-dash line is for  $M_{Z'} = 250 \text{ GeV}$ , and the dotted line is for  $M_{Z'} = 350 \text{ GeV}$ . The long-dashed lines represent  $1\sigma$  deviations from the standard model for an integrated luminosity of  $600 \text{ pb}^{-1}$  per polarization.

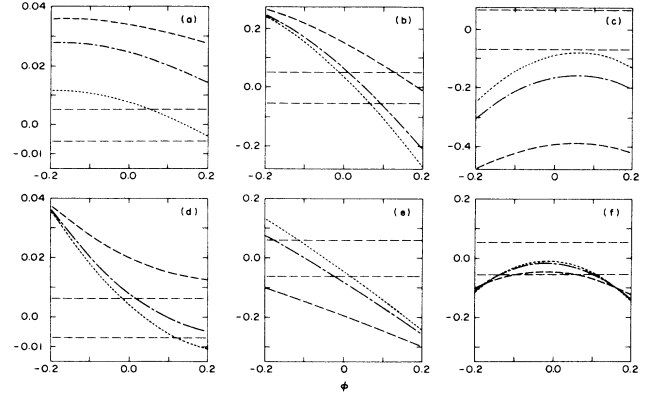


FIG. 7. Deviations from the standard model for the various  $ep$  asymmetries as a function of  $\phi$  for  $\theta_{E_6} = \theta_\eta$  and  $s = 64000 \text{ GeV}^2$ . The figure labeling is as in Fig. 6.

metries vary with the parameters of the extended model. With our crude error estimates one can see that HERA experiments should be able to measure the effects of a  $Z'$  with mass of several hundred GeV. One can take this information and translate it into a form which describes the reach of HERA in a more transparent fashion. In the extended model there are three free parameters once the ratio ( $g_{Z'}/g_{Z_0}$ ) has been fixed so in general the  $M_{Z'}$  mass limit would be a two-dimensional surface which depended on  $\phi$  and  $\theta_{E_6}$ . We will limit ourselves to two slices in this three-dimensional space. In the first we take  $\theta_{E_6} = \theta_\eta$ , which is popular in superstring-motivated models, and see how the limit on  $M_{Z'}$  varies with  $\phi$  and in the second we set  $\phi = 0$  and see how the limit on  $M_{Z'}$  varies with  $\theta_{E_6}$ . Once the experimental errors on  $M_{Z_0}$  and  $M_W$  are reduced one could eliminate  $\phi$  as a free parameter and redo

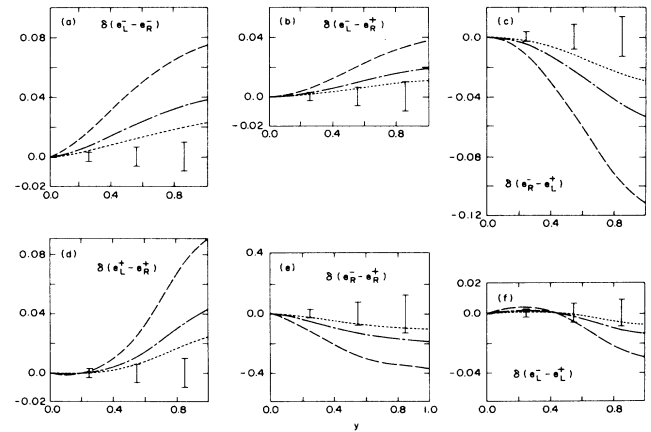


FIG. 8. Deviations from the standard model for the various  $ep$  asymmetries as a function of  $y$  for  $\theta_{E_6} = \theta_\eta$ ,  $\phi = 0$ , and  $s = 64000 \text{ GeV}^2$  obtained by integrating  $d\sigma/(dx dy)$  over  $x$  from 0.1 to 1. The figure labeling is as in Fig. 6 with the error bars determined as in Fig. 4.

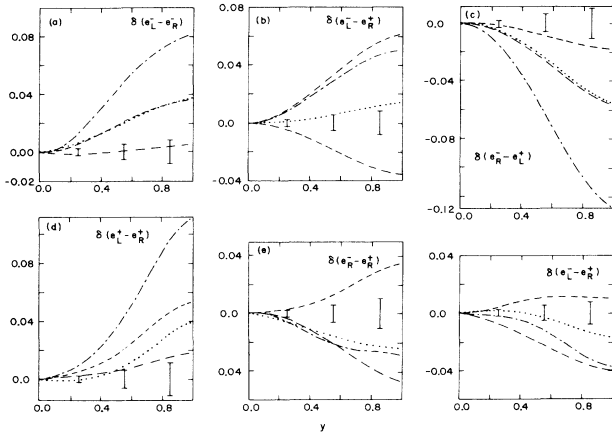


FIG. 9.  $\delta(\alpha-\beta)$  for some representative parameter sets allowed by present experimental bounds. The line labeling is as in Fig. 5 with the error bars determined as in Fig. 4.

the second plot with an error for  $M_{Z'}$  reflecting the uncertainty in  $M_{Z^0}$  and  $M_{Z_{SM}}$ . The criteria we use in determining the largest observable  $Z'$  mass for a given value of  $\phi$  or  $\theta_{E_6}$  is that the deviation of a measured quantity lies outside the 95% confidence limit of the standard model. We determine the statistical error in the standard model for  $s = 64000 \text{ GeV}^2$  with an integrated luminosity of  $600 \text{ pb}^{-1}$  per polarization which for the expected HERA luminosity represents about 160 days total running time.

In Fig. 10 we show the limit on  $M_{Z'}$  vs  $\phi$  for the case of  $\theta_{E_6} = \theta_\eta$ . The values allowed by low-energy neutral-current data at the 90% C.L. as determined by Durkin and Langacker<sup>7</sup> are given by the region inside the solid curve. Improvements in the  $W$  mass measurement relative to the  $Z^0$  expected at the next generation of hadron collider experiments will further restrict the allowed parameter space to lie inside the region bounded by the dashed curves given by Franzini and Gilman.<sup>13</sup> Finally, left-right-asymmetry measurements taken at the  $Z^0$  pole at SLC and LEP will be able to measure  $\phi$  to the accuracy given by the dot-dash curves assuming  $10^5 Z^0$ s are produced. We note that the latter measurements are almost totally insensitive to the mass of a  $Z'$  boson. Measurements of the forward-backward or left-right asymmetry off the  $Z^0$  pole at KEK TRISTAN, SLC, or LEP will not further restrict the allowed region of the  $M_{Z'}-\phi$  plane but if deviations from the standard model are observed these measurements will be important in determining the parameters of the  $Z'$ , given the insensitivity of the measurements at the  $Z^0$  pole to  $M_{Z'}$ . To these curves we add two representative curves of measurements which will be made at HERA,  $\sigma(e_L^-) - \sigma(e_R^-)$  and  $\sigma(e_R^-) - \sigma(e_L^+)$ . These measurements can probe the  $Z'$  mass to over 300 GeV in regions not probed by other experiments. Given that deviations are observed, the four other asymmetries and  $\sigma(e^-)$  and  $\sigma(e^+)$  will be important in determining the parameters of the  $Z'$  boson.

In Fig. 11 we repeat the exercise, this time fixing  $\phi = 0$  and varying  $\theta_{E_6}$ . The region under the solid curve

represents the parameter space ruled out by existing neutral-current data. To obtain this curve we follow London and Rosner<sup>6</sup> with the two following changes: we use  $M_{Z^0} = 92.3 \pm 1.7 \text{ GeV}$  and  $M_W = 80.8 \pm 1.4 \text{ GeV}$  (Ref. 22) and the value for atomic parity violation in cesium of  $Q_W(\text{Cs}) = -71.7 \pm 5.8$  (Ref. 23). The region under the dashed curve represents the region which TRISTAN can probe with measurements in  $e^+e^-$  of the left-right asymmetry  $A_{LR}$  at  $\sqrt{s} = 60 \text{ GeV}$ , with  $L = 10^{31} \text{ cm}^{-2} \text{ sec}^{-1}$  per polarization for a running time of  $10^7$  sec, and again the criterion that any deviation must lie outside the 95% C.L. of the standard model. The dash-dot curve is the region which can be probed at SLC/LEP using  $A_{LR}$  for  $\sqrt{s} = 110 \text{ GeV}$  with the same integrated luminosity giving  $10^6 Z^0$ s at the  $Z^0$  pole, again assuming deviations greater than the 95% C.L. To this we add our results for the range of  $M_{Z'}$  that can be probed at HERA using the same criteria as above. We show the  $\sigma(e_L^-) - \sigma(e_R^+)$  and  $\sigma(e_L^-) - \sigma(e_R^-)$  asymmetries which are given by the dotted and short-dash-long-dash curves, respectively. One can see that such measurements will extend the explored region considerably. Because of the nature of  $ep$  collisions it is nontrivial to extract the best possible bounds for a given set of data and we have presented the results of

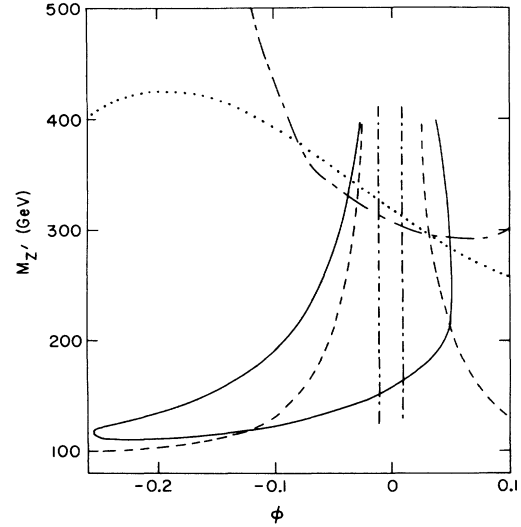


FIG. 10. The 95%-confidence-limit bounds for an extra  $Z'$  with  $\theta_{E_6} = \theta_\eta$  as a function of  $\phi$ . The area inside the solid line represents the region in  $M_{Z'}-\phi$  parameter space allowed by existing neutral-current data as given by Durkin and Langacker in Ref. 7, the region outside the dashed curves represents the parameter values which would be probed by measuring  $M_W$  to 500 MeV as given by Franzini and Gilman in Ref. 13, the region outside the dot-dash curves represents the parameter space which can be probed by measuring the left-right asymmetry in  $e^+e^-$  annihilation at the  $Z^0$  pole with  $10^5 Z^0$ s, the region under the dotted curve represents the region probed by the  $\sigma(e_L^-) - \sigma(e_R^-)$  asymmetry in  $ep$  collisions and the region under the short-dash-long-dash curve represents the region probed by  $\sigma(e_R^-) - \sigma(e_L^+)$  asymmetry in  $ep$  collisions. The criteria for these limits are given in the text.

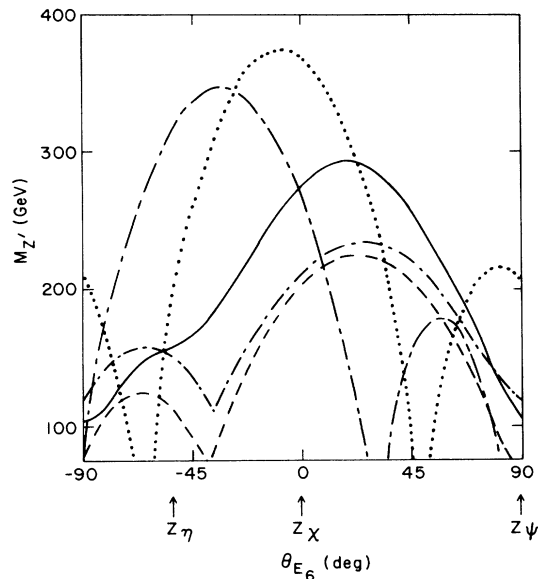


FIG. 11. The 95%-confidence-limit bounds for the mass of a  $Z'$  as a function of  $\theta_{E_6}$  with  $\phi=0$ . The area under the solid curve represents the region already ruled out by existing neutral-current data, the region under the dashed curve represents the region which can be probed by  $e^+e^-$  collisions at TRISTAN, the region under the dot-dash curve represents the region that can be probed by  $e^+e^-$  at SLC/LEP with  $\sqrt{s}=110$  GeV for the same integrated luminosity giving  $10^6$   $Z^0$ 's at the  $Z^0$  pole, the region under the dotted curve represents the parameter space that can be probed by the  $\sigma(e_L^-)-\sigma(e_R^+)$  asymmetry in  $ep$  collisions at HERA, and the region under the short-dash-long-dash curve represents the parameter space that can be probed by the  $\sigma(e_L^-)-\sigma(e_R^-)$  asymmetry at HERA. The criteria determining these limits are given in the text.

what we believe to be a reasonable, but nevertheless simplistic strategy. Given more sophisticated analysis techniques it is possible that the maximum  $Z'$  mass that can be detected would be larger than the bounds we have presented here.

#### IV. CONCLUSIONS

In this paper we have studied the effect of an extra neutral gauge boson on cross sections and asymmetries in  $ep$

colliders. We have found that deviations from the standard model allowed by present experimental data are large although it is likely that new data from the  $e^+e^-$  colliders SLC and LEP will change these limits, either by improving them or by observing deviations from the standard model.

Nevertheless  $ep$  physics will contribute to our understanding of extra  $Z^0$  bosons should they exist. This is because in  $e^+e^-$  collisions the first hint of new physics is likely to manifest itself as deviations from the standard model at the  $Z^0$  pole where the statistics will be greatest. However, at the  $Z^0$  pole it is not possible to extract the values of  $\theta_{E_6}$  and  $\phi$  simultaneously. To do so one must make measurements at a different value of  $s$  where the statistics will be much poorer. Thus even if evidence for an extra neutral gauge boson is observed in  $e^+e^-$  collisions the complementary measurements at HERA will be necessary to determine its parameters. On the other hand, if no such evidence exists, it does not rule out the existence of an extra neutral gauge boson, only that its mixing with the standard-model  $Z^0$  is small. In this case it is still possible that HERA will discover a  $Z'$  that has thus far eluded observation.

Our conclusion is that measurements in  $ep$  collisions at HERA will be a powerful tool in either detecting the presence of an extra neutral gauge boson, or if one has already been discovered, in measuring its parameters. In combination with  $e^+e^-$  measurements it should be possible to explore mass scales of up to several hundred GeV for the existence of an extra  $E_6$  neutral gauge boson.

#### ACKNOWLEDGMENTS

The authors are most grateful to Genevieve Belanger and David London for the computer program used to obtain the bounds from neutral-current data. S.G. thanks Genevieve Belanger, R. Cashmore, David London, Bill Marciano, and John Martin for helpful conversations and the Department of Physics at the University of Toronto for their hospitality during the course of this work. This work was partially funded by the Natural Science and Engineering Research Council of Canada. This work was supported in part by the U.S. Department of Energy under Contract No. DE-AC02-76CH00016.

\*Present address.

<sup>1</sup>M. Green and J. Schwarz, Phys. Lett. **149B**, 117 (1984); **151B**, 21 (1985).

<sup>2</sup>E. Witten, Phys. Lett. **155B**, 1551 (1985); Nucl. Phys. **B258**, 75 (1985); P. Candelas, G. T. Horowitz, A. Strominger, and E. Witten, *ibid.* **B258**, 46 (1985); M. Dine, W. Kaplunovsky, M. Mangano, C. Nappi, and N. Seiberg, *ibid.* **B259**, 549 (1985).

<sup>3</sup>J. Ellis *et al.*, Nucl. Phys. **B276**, 14 (1986); Mod. Phys. Lett. **A1**, 57 (1986); J. D. Breit, B. A. Ovrut, and G. C. Segrè, Phys. Lett. **158B**, 33 (1985); S. Cecotti *et al.*, *ibid.* **156B**, 318 (1985).

<sup>4</sup>R. W. Robinett, Phys. Rev. D **33**, 1908 (1984); V. Barger, N.

Deshpande, R. J. N. Phillips, and K. Whisnant, *ibid.* **33**, 1912 (1986); T. G. Rizzo, *ibid.* **34**, 1438 (1986).

<sup>5</sup>J. Rosner, Comments Nucl. Part. Phys. **15**, 195 (1986).

<sup>6</sup>D. London and J. Rosner, Phys. Rev. D **34**, 1530 (1986).

<sup>7</sup>L. S. Durkin and P. Langacker, Phys. Lett. **166B**, 436 (1986).

<sup>8</sup>V. Barger, N. G. Deshpande, and K. Whisnant, Phys. Rev. Lett. **56**, 30 (1986); S. M. Barr, *ibid.* **55**, 2778 (1985); E. Cohen, J. Ellis, K. Enqvist, and D. V. Nanopoulos, Phys. Lett. **165B**, 76 (1985).

<sup>9</sup>W. J. Marciano and A. Sirlin, Phys. Rev. D **35**, 1672 (1987).

<sup>10</sup>J. L. Rosner, Phys. Rev. D **35**, 2244 (1987); V. Barger, N. G. Deshpande, J. L. Rosner, and K. Whisnant, *ibid.* **35**, 2893

- (1987); F. del Aguila, M. Quiros, and F. Zwirner, CERN Report No. CERN-TH.4536/86, 1986 (unpublished); D. London and J. Rosner, Phys. Rev. D **34**, 1530 (1986).
- <sup>11</sup>For early work, see W. Hollik, Z. Phys. C **8**, 149 (1981); W. Hollik and A. Zepeda, *ibid.* **12**, 67 (1982).
- <sup>12</sup>G. Bélanger and S. Godfrey, Phys. Rev. D **34**, 1309 (1986); **35**, 378 (1987).
- <sup>13</sup>P. J. Franzini and F. J. Gilman, Phys. Rev. D **35**, 855 (1987).
- <sup>14</sup>V. D. Angelopoulos, J. Ellis, D. V. Nanopoulos, and N. Tracos, Phys. Lett. **176B**, 203 (1986).
- <sup>15</sup>F. del Aguila, M. Quiros, and F. Zwirner, CERN Report No. CERN-TH.4506/86, 1986 (unpublished); I. Bigi and M. Cvetič, Phys. Rev. D **34**, 1651 (1986); T. Rizzo *ibid.* **34**, 2699 (1986); M. Cvetič and B. Lynn, *ibid.* **35**, 51 (1987); C. Vaz and D. Wurmser, *ibid.* **33**, 2578 (1986); J. P. Ader, S. Narison, and J. C. Wallet, Phys. Lett. **176B**, 215 (1986).
- <sup>16</sup>For a recent review of *ep* physics, see R. Cashmore *et al.*, Phys. Rep. **122C**, 275 (1985). See also J. A. Bagger and M. E. Peskin, Phys. Rev. D **31**, 2211 (1985).
- <sup>17</sup>We note that Angelopoulos, Ellis, Nanopoulos, and Tracos (Ref. 14) have examined asymmetries in *ep* collisions for the so-called *minimal superstring model* (Ref. 3) which is a specific case of the present, more general analysis. See also F. Cor-net and R. Rückl, Phys. Lett. **184B**, 263 (1987).
- <sup>18</sup>P. Langacker, Phys. Rev. D **30**, 2008 (1984); Durkin and Langacker (Ref. 7).
- <sup>19</sup>See, for instance, R. W. Robinett, Phys. Rev. D **26**, 2388 (1982); R. W. Robinett and J. L. Rosner, *ibid.* **25**, 3036 (1982); **26**, 2396 (1982); P. Langacker, R. W. Robinett, and J. L. Rosner, *ibid.* **30**, 1470 (1984).
- <sup>20</sup>W. J. Marciano, in Proceedings of the Twenty-Third International Conference on High Energy Physics, Berkeley, California, 1986, edited by S. Loken (World Scientific, Singapore, to be published).
- <sup>21</sup>E. Eichten, I. Hinchliffe, K. D. Lane, and C. Quigg, Rev. Mod. Phys. **56**, 579 (1984).
- <sup>22</sup>S. Greer, in Proceedings of the Twenty-Third International Conference on High Energy Physics (Ref. 20); A. Roussarie, *ibid.*
- <sup>23</sup>C. Bouchiat and C. A. Piketty, LPTENS report, 1986 (unpublished); M. A. Bouchiat, J. Guena, and L. Pottier, J. Phys. (Paris) **46**, 1897 (1985); S. Gilbert, M. Noecker, R. Watts, and C. Wieman, Phys. Rev. Lett. **55**, 2680 (1985). We are most grateful to Bill Marciano for pointing out the importance of these measurements in obtaining bounds on  $M_Z$ .